Supplement of Atmos. Chem. Phys., 16, 3207–3225, 2016
http://www.atmos-chem-phys.net/16/3207/2016/
doi:10.5194/acp-16-3207-2016-supplement
© Author(s) 2016. CC Attribution 3.0 License.

Atmospheric Chemistry and Physics Open Access EGU

Supplement of

New insights into $PM_{2.5}$ chemical composition and sources in two major cities in China during extreme haze events using aerosol mass spectrometry

Miriam Elser et al.

Correspondence to: Ru-Jin Huang (rujin.huang@ieecas.cn), Imad El-Haddad (imad.el-haddad@psi.ch) and André S. H. Prévôt (andre.prevot@psi.ch)

The copyright of individual parts of the supplement might differ from the CC-BY 3.0 licence.

Table S1: Squared Pearson coefficient (top) and ratios (bottom) derived from the correlations between the OA sources and its external time series for the four periods of interest as represented in Fig. S8. The values reported in parenthesis are related to the unconstrained source apportionment solution (average of 10 runs).

R^2	Xi'an		Beijing		Overall
	Extreme haze	Reference	Extreme haze	Reference	
OOA vs. NH_4	0.22 (0.50)	0.71 (0.83)	0.38 (0.63)	0.60 (0.53)	0.88 (0.92)
COA vs. $C_6H_{10}O$	0.21 (0.008)	0.58 (0.29)	0.44 (0.2)	0.71 (0.53)	0.31 (0.39)
CCOA vs. AMS-PAH	0.57 (0.61)	0.59 (0.60)	0.96 (0.97)	0.96 (0.97)	0.62 (0.63)
BBOA vs. $C_2H_4O_2$	0.98 (0.96)	0.96 (0.88)	0.79 (0.80)	0.81 (0.78)	0.97 (0.96)
BBOA vs. eBC_{wb}	0.33 (0.34)	0.53 (0.53)	N.A.	N.A.	0.38 (0.38)
HOA vs. eBC_{tr}	0.61 (0.67)	0.61 (0.62)	N.A.	N.A.	0.61 (0.63)

Ratio	Xi'an		Beijing		Overall
(source/marker)	Extreme haze	Reference	Extreme haze	Reference	
OOA/NH_4	0.99 (0.74)	1.08 (0.64)	0.67 (0.42)	0.76 (0.31)	0.97 (0.70)
COA/$C_6H_{10}O$	60 (219)	144 (267)	126 (372)	198 (304)	96 (243)
CCOA/AMS-PAH	3.4 (2.4)	5.5 (3.3)	10.8 (8.4)	10.4 (7.9)	7.2 (5.2)
BBOA/$C_2H_4O_2$	51 (39)	54 (39)	29 (34)	22 (28)	51 (39)
BBOA/eBC_{wb}	10.8 (8.3)	4.9 (3.6)	N.A.	N.A.	7.3 (5.5)
HOA/eBC_{tr}	1.18 (0.62)	1.6 (2.6)	N.A.	N.A.	1.27 (0.63)

Table S2: Mean concentration and standard deviation for all measured compounds and sources for the four periods of interest.

Mean conc.	Xi'an		Beijing	
($\mu g\ m^{-3}$)	Extreme haze	Reference	Extreme haze	Reference
$PM_{2.5}$	537 ± 146	140 ± 99	243 ± 47	75 ± 61
OA	216 ± 85	76 ± 56	103 ± 33	42 ± 37
SO_4	119 ± 30	12 ± 12	47 ± 15	12 ± 11
NO3	71 ± 12	14 ± 11	43 ± 11	7.4 ± 5.6
NH4	31 ± 15	11.4 ± 10.6	14.9 ± 5.1	5.3 ± 5.4
Cl	62 ± 12	11.3 ± 9.0	35.4 ± 7.9	8.4 ± 6.6
eBC	39 ± 16	15.0 ± 9.5	3.4 ± 1.1	1.5 ± 1.3
OOA	47 ± 12	5.4 ± 8.9	14.7 ± 5.5	2.4 ± 3.1
HOA	49 ± 41	23 ± 27	12.9 ± 9.0	6.9 ± 9.9
BBOA	67 ± 40	22 ± 20	15.1 ± 9.6	4.6 ± 6.9
CCOA	7.7 ± 8.0	5.7 ± 4.1	33 ± 23	16 ± 18
COA	33 ± 16	15.8 ± 8.7	19 ± 10	10.0 ± 9.6
PAH	3.5 ± 2.2	1.6 ± 1.1	4.0 ± 2.7	1.9 ± 2.2

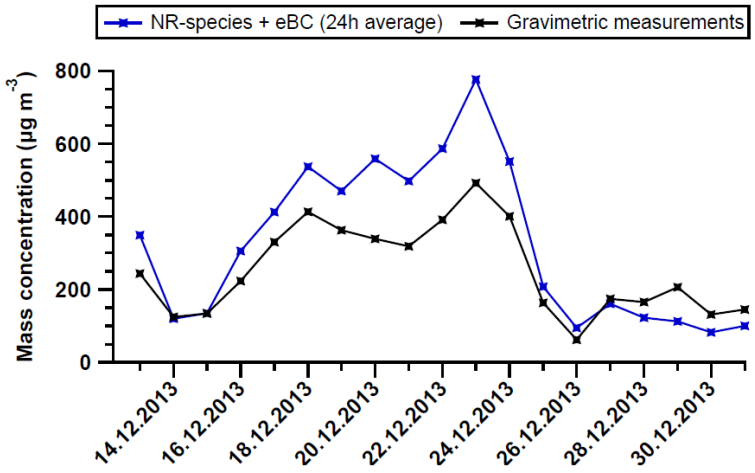

Figure S1. Comparison between mass concentrations obtained from gravimetric measurements of $PM_{2.5}$ filters (black) and total mass measured with AMS and Aethalometer (blue); Gravimetric analysis only available for the first part of measurements in Xi'an.

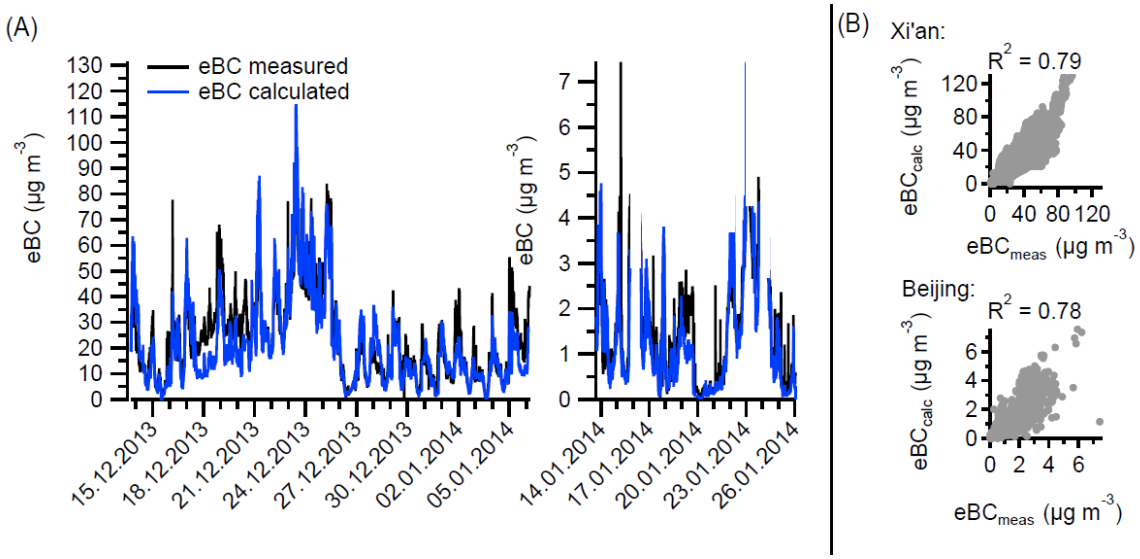

Figure S2. (a) Time series of the measured eBC (black) and the eBC calculated (blue) as a linear combination of HOA, BBOA and CCOA for the full measurements period. (b) Correlation between measured and calculated eBC in Xi'an (top) and Beijing (bottom).

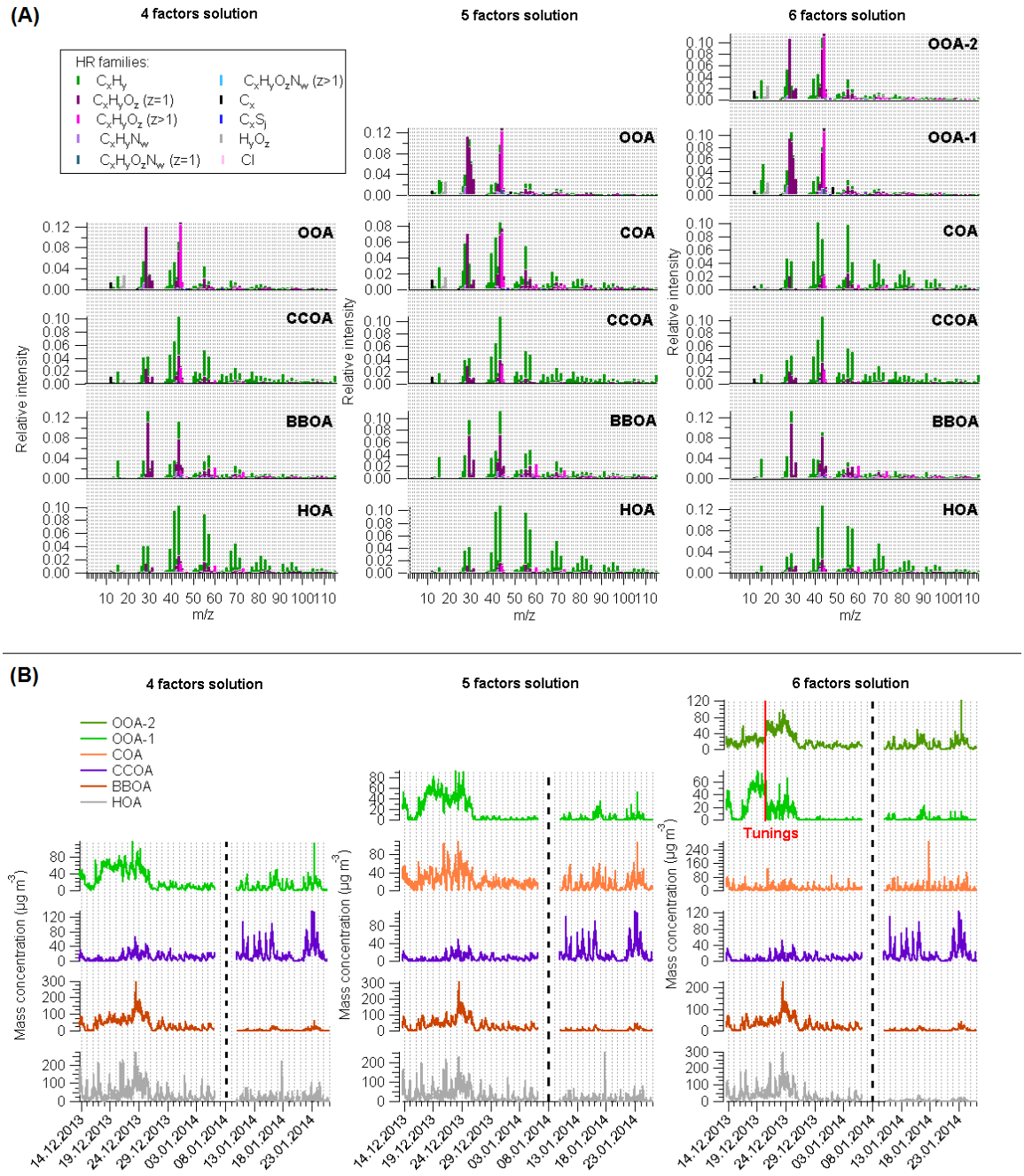

Figure S3. (a) PMF profiles for four, five and six factor solution (from left to right); (b) Time series of the identified profiles for four, five and six factors (from left to right).

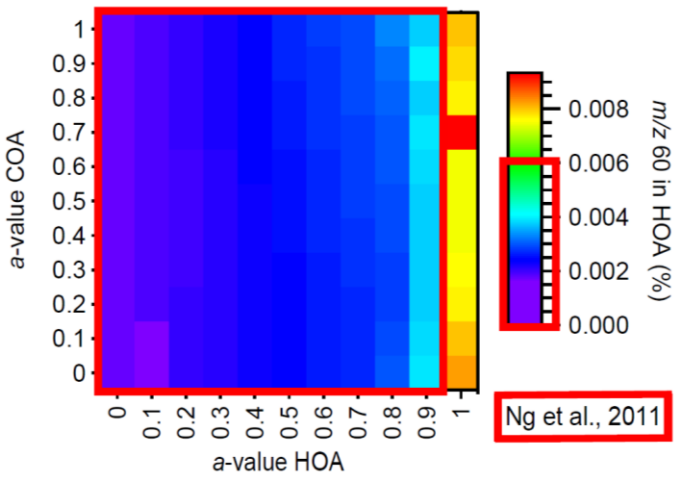

Figure S4. Relative contribution of *m/z* 60 in HOA profile over the investigated *a* value space; Acceptable contributions according to Ng et al. (2011) inside red area (mean ± 2σ).

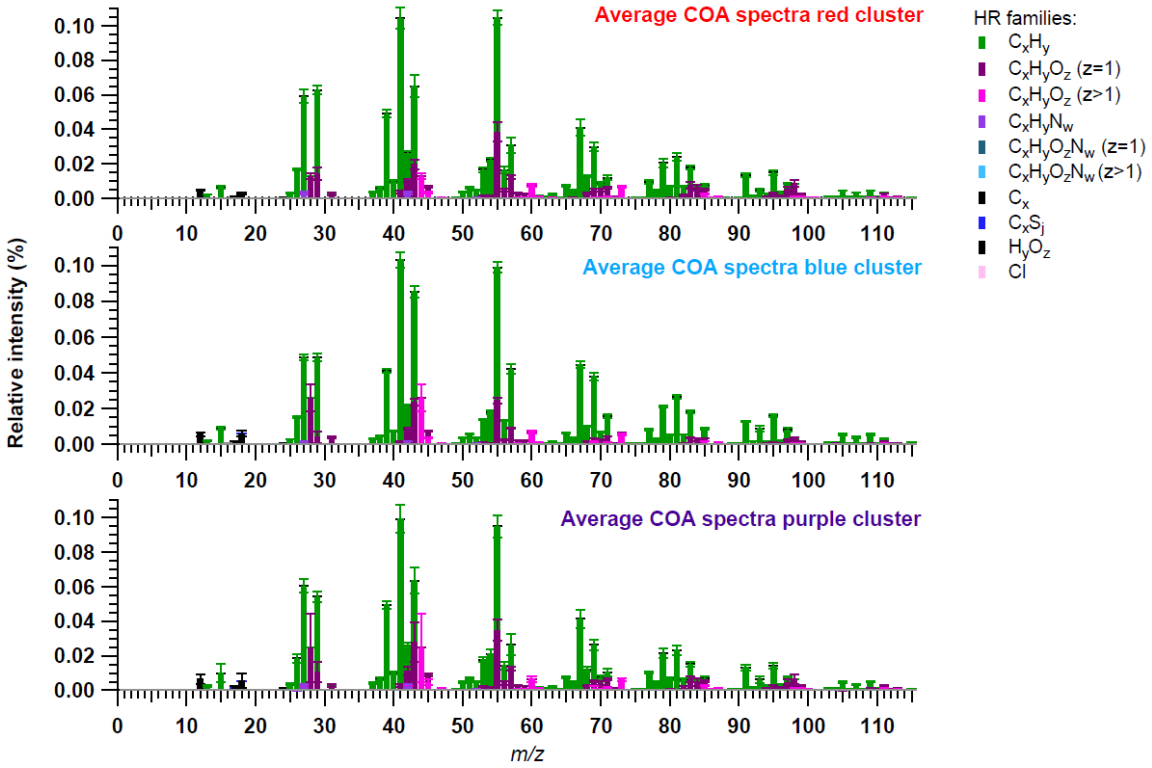

Figure S5. Averaged COA mass spectra for red cluster (top), blue cluster (center) and purple cluster (bottom) of the three clusters solution shown in Fig. 1. The error bars represent the standard deviation among all solutions in the final *a* value range.

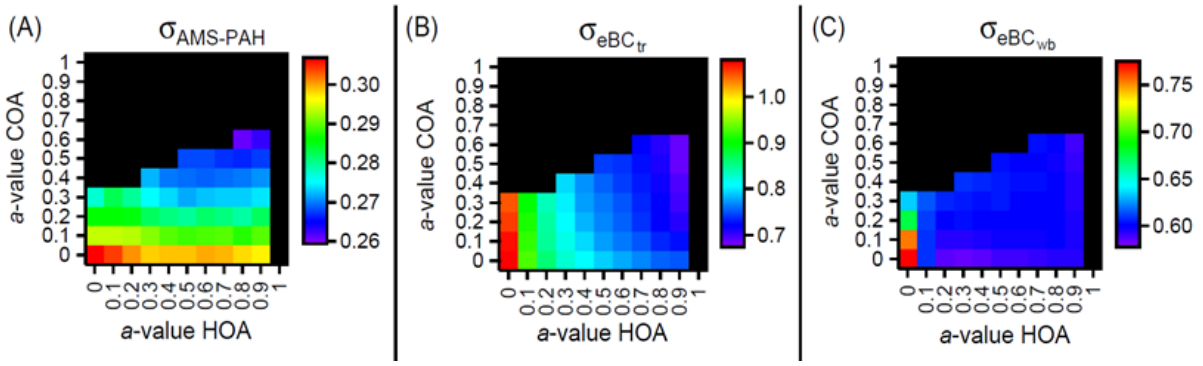

Figure S6. Investigated *a* value space with color code showing the standard deviation of the normalized difference between the measured external time series and their fits calculated using the source apportionment results for: (a) AMS-PAH and BBOA, CCOA and HOA; (b) eBC_{tr} and HOA; (c) eBC_{wb} and BBOA.

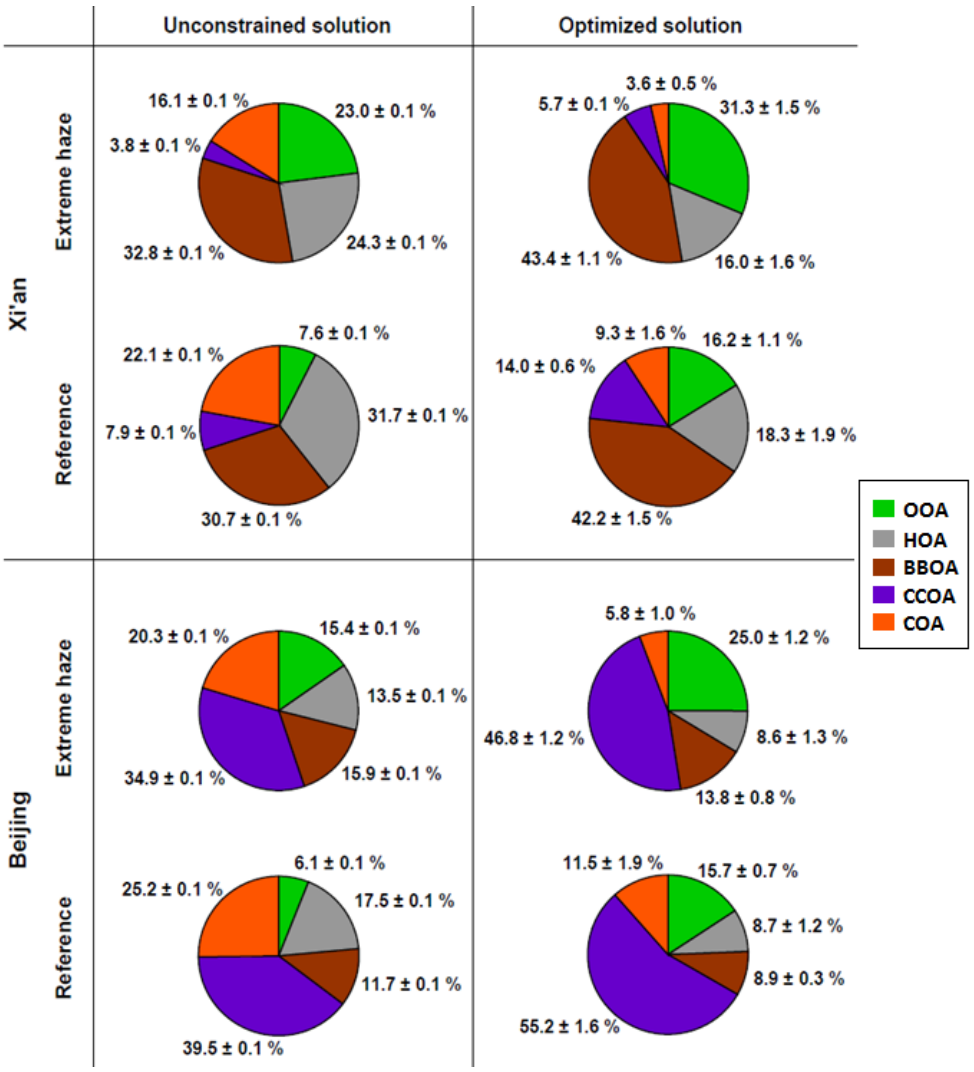

Figure S7: Comparison of the unconstrained and optimized solutions in terms of the relative contributions of the OA sources for the four periods of interest.

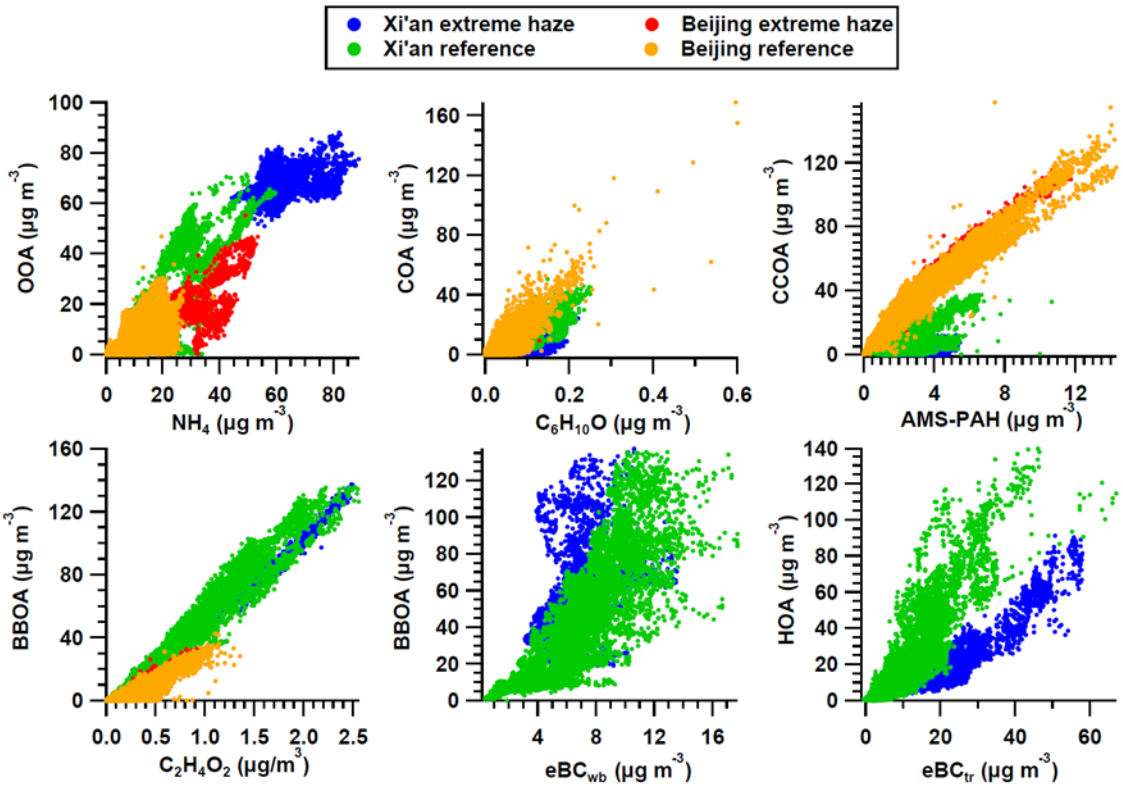

Figure S8. Scatter plots between OA sources from the optimized solution and their external tracers; Colors are used to indicate the different periods of interest.

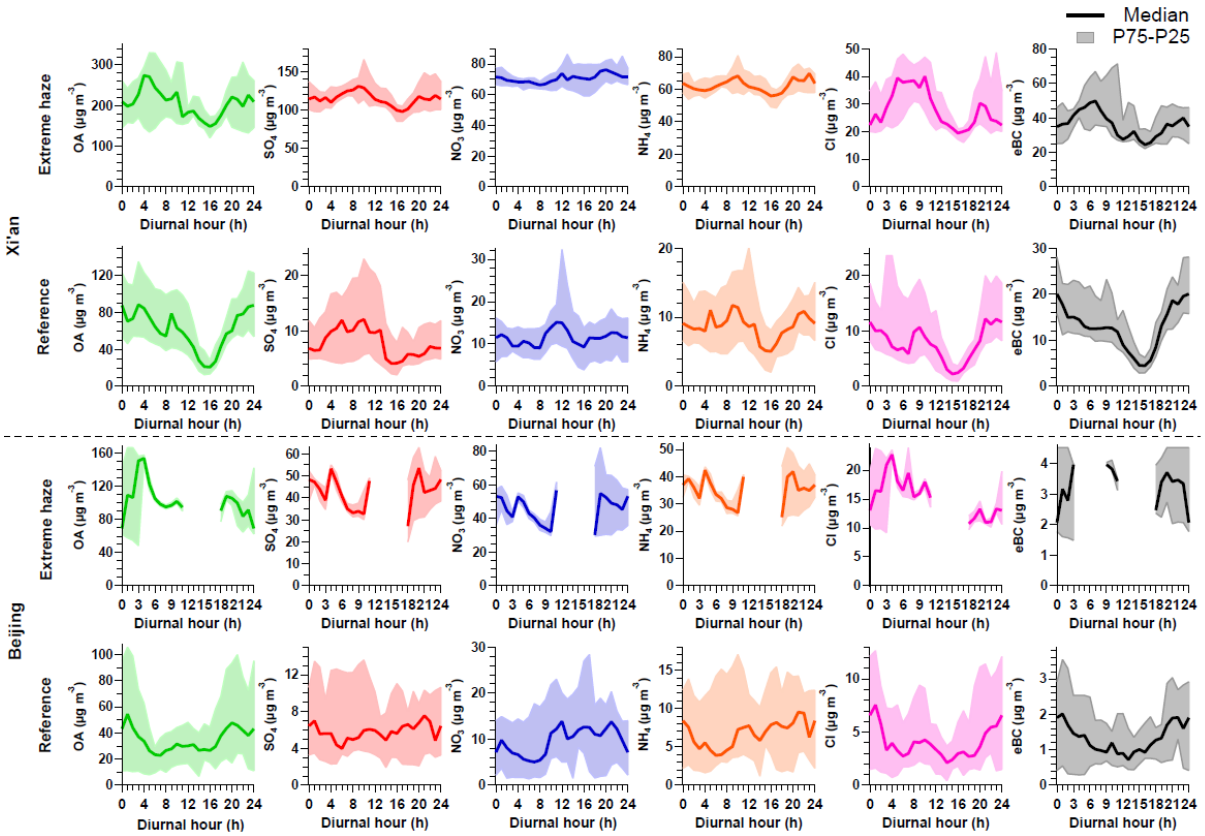

Figure S9. Median diurnal trends for AMS species and eBC during the four periods of interest. Shaded area represents the 25th and 75th percentiles (P25 and P75) of the diurnals.

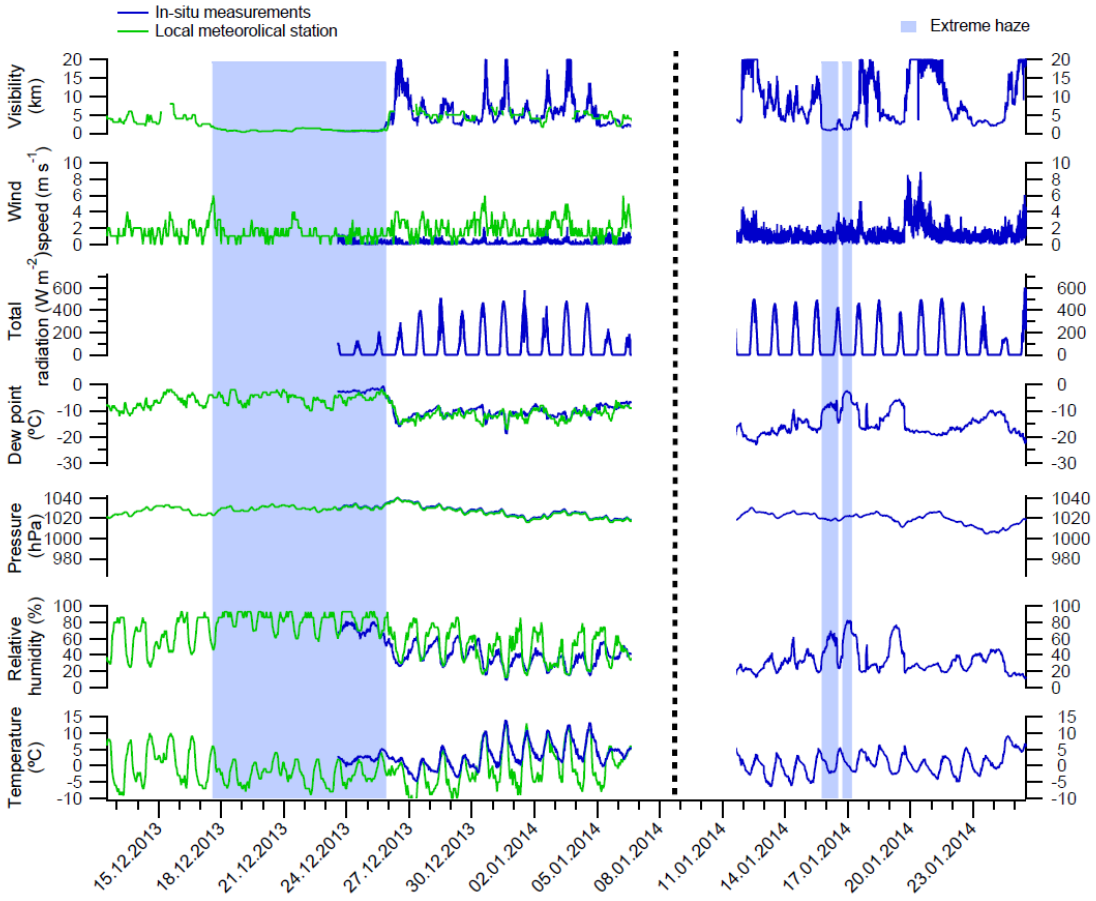

Figure S10. Meteorological parameters during the measurement periods including visibility, wind speed, total radiation, net radiation, dew point, pressure, relative humidity and temperature (from top to bottom); Blue time series were retrieved in situ in the measurement locations and green time series were recorded in nearby local meteorological stations.

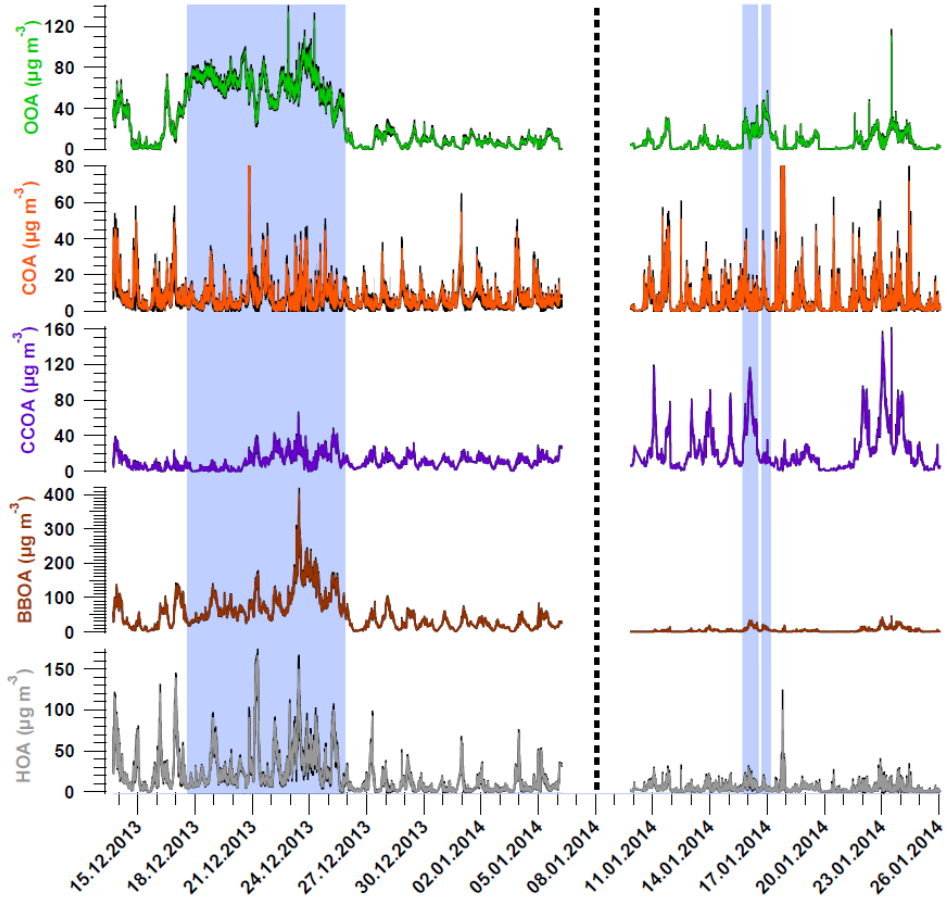

Figure S11. Time series of the OA sources with black shadow representing the standard deviation among all good *a* value combinations.

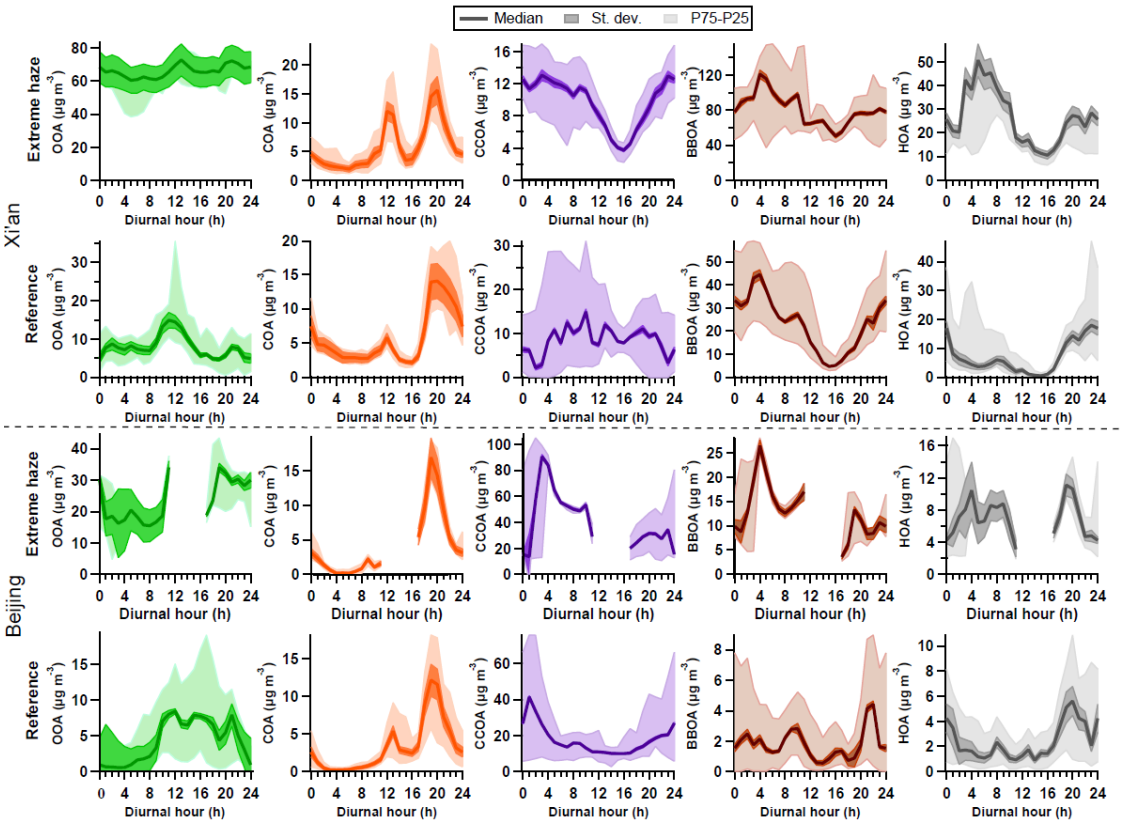

Figure S12. Median diurnal trends for OA sources during the four periods of interest. Light shaded area represents the 25th and 75th percentiles (P25 and P75) and strong shaded area represents the standard deviation among all good *a* value combinations.

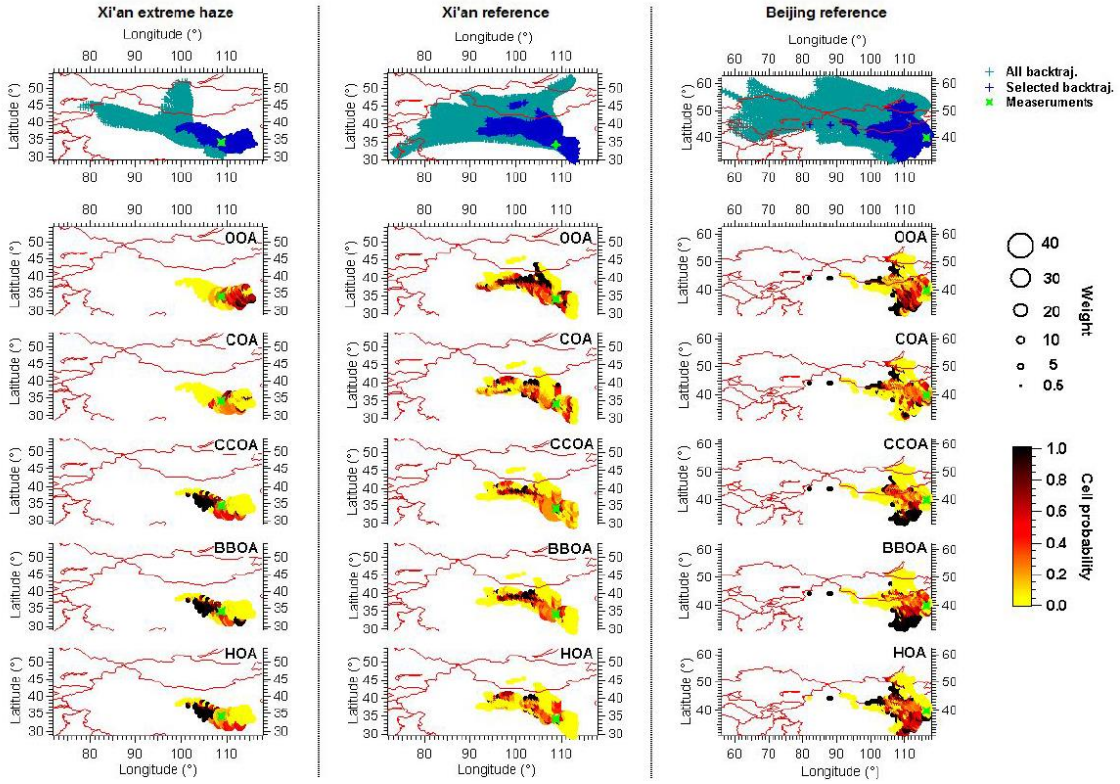

Figure S13. Source regions of the OA sources identified with PSCF analysis for 3 periods of interest (the period with extreme haze in Beijing has too few points for statistically significant PSCF analysis). The color code indicates the normalized cell probability averaged for the 3 possible back-trajectory heights (i.e. the probability that a certain pollutant was originated from a certain cell). The marker size is given by a weighting factor that takes into account the standard deviation from results at different heights and the back-trajectory counting statistic error. A detailed description of the PSCF methodology can be found in Polissar et al. (1999). The analyses were performed on 72-h wind back-trajectories calculated at 3 different altitudes above the receptor site (i.e. 100, 500, and 1000 m). The backward air mass trajectories were calculated using Hybrid Single-Particle Lagrangian Integrated Trajectory (HYSPLIT4; Draxler and Hess, 1998) with a time resolution of 1 hour. Precipitation was taken into account by considering that rain above 0.1 mm h^{-1} (Bressi et al., 2014) will result in the wet deposition of the pollutant. An altitude threshold was set to 500 m (Sensitivity analyses performed by setting this threshold to 500 m, 1000 m and 1500 m above ground, indicate that the results are not significantly affected by this parameter) and a lower mass threshold corresponding to the 75^{th} percentile (P75) was used for the mass concentrations (this threshold was tested at P50, P75 and P90; results were found to be similar at P50 and P75, while using P90 did not provide statistically robust results).

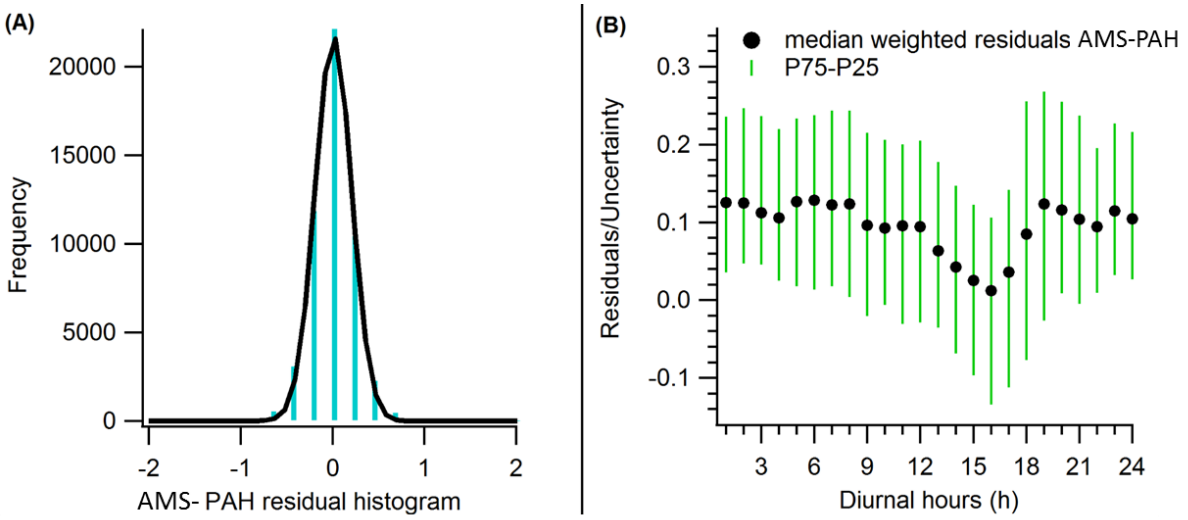

Figure S14: (a) Weighted AMS-PAH residuals histogram (blue distribution) and Gaussian fit (black curve); (b) Diurnal variation of weighted AMS-PAH residuals.

References

Bressi, M., Sciare, J., Ghersi, V., Mihalopoulos, N., Petit, J.-E., Nicolas, J. B., Moukhtar, S., Rosso, A., Féron, A., Bonnaire1, N., Poulakis, E., and Theodosi, C.: Sources and geographical origins of fine aerosols in Paris (France), Atmos. Chem. Phys., 14, 8813–8839, 2014.

Draxler, R. and Hess, G. D.: An overview of the HYSPLIT 4 modeling system for trajectories, dispersion and deposition, Aust. Meteor. Mag., 47, 295–308, 1998.

HYSPLIT4: Hybrid single-particle Lagrangian integrated trajectory model, NOAA Air Resources Laboratory: http://www.arl.noaa.gov/ready/hysplit4.html, last access: 25 May 2015.

Ng, N. L., Canagaratna, M. R., Jimenez, J. L., Zhang, Q., Ulbrich, I. M., and Worsnop, D. R.: Real-time methods for estimating organic component mass concentrations from aerosol mass spectrometer data, Environ. Sci. Technol., 45, 910–916, 2011.

Polissar, A. V., Hopke, P. K., Paatero, P., Kaufmann, Y. J., Hall, D. K., Bodhaine, B. A., Dutton, E. G., and Harris, J. M.: The aerosol at Barrow, Alaska: long-term trends and source locations, Atmos. Environ., 33, 2441–2458, 1999.